Journal of Zhejiang University-SCIENCE A (Applied Physics & Engineering)
ISSN 1673-565X (Print); ISSN 1862-1775 (Online)
www.zju.edu.cn/jzus; www.springerlink.com
E-mail: jzus@zju.edu.cn

One and two dimensional chloride ion diffusion of fly ash concrete under flexural stress*

Yun-sheng ZHANG†, Wei SUN, Zhi-yong LIU, Shu-dong CHEN
(*Jiangsu Key Laboratory for Construction Materials, Southeast University, Nanjing 211189, China*)
†E-mail: zhangys279@163.com

Received Jan. 15, 2011; Revision accepted June 7, 2011; Crosschecked Aug. 19, 2011

Abstract: A preloading frame is firstly designed to accurately apply external flexural stress to concrete specimens. Then a method is developed to measure one and two dimensional (1D and 2D) chloride ion concentrations at different distances from the surface of concrete under flexural stress. Using this method and the preloading frame, 1D and 2D stress-diffusion is systematically investigated for fly ash concretes made with different fly ash contents (0%, 10%, 20%, 40%, and 60%), and water to binder ratios (0.3, 0.35, and 0.4). The stress accelerating effect on 1D and 2D chloride ion diffusion is also quantitatively analyzed through a comparison between stress-diffusion and nonstress-diffusion. A diffusion accelerating effect caused by external flexural stress can clearly be observed through the comparison. In order to quantify the stress accelerating effect, a stress accelerating factor is proposed in this paper. The relationship between stress accelerating factor and external stress-to-ultimate stress ratio is given as an exponential function. Finally, the process of the initiation, prorogation, and distribution of microcracks on the tensile face of specimen is observed in-situ by using a small-sized loading frame and scanning electron microscope (SEM). The above research provides an insight into chloride attack on the edge reinforcing bars of concrete structures under flexural stress, such as large-span beam and board in the field of civil engineering.

Key words: Fly ash, Concrete, Flexural stress, Chloride ion, One and two dimension
doi:10.1631/jzus.A1100006 **Document code:** A **CLC number:** TU528

1 Introduction

Chloride ion induced corrosion is a primary cause of the durability deterioration in reinforced concrete structures (Mehta, 1997). Since the 1960s, studies on chloride ion diffusion in concrete have been becoming a topic of interest in the area of concrete structural durability. Many experimental results and conclusions about chloride ion diffusion characteristics in concrete have been obtained and successfully applied in the service life prediction of field concrete structures (Tang and Nilsson, 1993; Maage *et al.*, 1996; Mehta, 1997; Weyers, 1998; Liang *et al.*, 1999; 2009; Khatri and Sirivivatnanon, 2004; Friedmann *et al.*, 2004; 2008; Suwito and Xi, 2008; Darmawan, 2010). However, it can be found that these observations are mostly obtained by one dimensional (1D) diffusion tests on concrete exposed to chloride salt solution. As it is well known, some important locations of the field concrete structures such as the corners or edges of beams and columns are subjected to the simultaneous attack of two dimensional (2D) chloride ion flows. The 2D diffusion of the edge concrete is quite different from 1D diffusion of the other locations. In practical engineering, the diffusion rate and depth of the edge concrete exposed to 2D chloride ion flows are much larger than those of the other concretes only exposed to 1D chloride ion flow. The steel bars embedded in the edge concrete

* Project supported by the National Basic Research Program (973) of China (No. 2009CB623200), the Doctoral Fund of Ministry of Education of China (No. 20100092110029), the Program for New Century Excellent Talents in University (No. NCET-08-0116), and the Guangxi Key Laboratory of Disaster Prevention and Reduction (No. 2008TM KF009), China

are easily corroded initially, which can be found in many investigative reports across the world (Maage *et al.*, 1996; Zhang *et al.*, 2011). Thus, it is very important to study the 2D diffusion of concrete exposed to chloride salt solution. In addition, concrete structures normally bear certain levels of loads in actual operations. Consequently, the chloride ion induced corrosion of the field concretes should be a consequence of the combined actions of loads and 1D or 2D chloride ion diffusion. In addition, use of fly ash as a cement replacement material has become common practice in marine concrete structure in recent years (Dhir and Jones, 1999; Thomas and Bamforth, 1999; Montemor *et al.*, 2002; Choi *et al.*, 2006; Chalee *et al.*, 2007; Chindaprasirt *et al.*, 2007; Rukzon and Chindaprasirt, 2008). Fly ash is used in concrete for economical and environmental reasons. Moreover, the fly ash particles react with calcium hydroxide producing hydration products that strongly decrease concrete porosity. This leads to smaller chloride diffusivity and higher resistivity, and therefore, the fly ash concrete are less susceptible to the ingress of harmful chloride ions. There are some long-term field and laboratory studies of chloride ingress in fly ash concrete (Dhir and Jones, 1999; Thomas and Bamforth, 1999; Montemor *et al.*, 2002; Choi *et al.*, 2006; Chalee *et al.*, 2007; Chindaprasirt *et al.*, 2007; Mien *et al.*, 2009; Rukzon and Chindaprasirt, 2009). Whereas few papers are available on 1D chloride ion diffusion of fly ash concrete under loads, not to mention 2D diffusion under loads (Dhir and Jones, 1999; Thomas and Bamforth, 1999; Chalee *et al.*, 2007; Chindaprasirt *et al.*, 2007).

2 Materials and methods

2.1 Materials

A Chinese standard (GB175, 2007) graded 42.5 P II type Portland cement with the compressive strength of 47.6 MPa at 28 d is used, similar to ASTM C150 (2005) type II cement.

Grade I fly ash (GB/T1596, 2005), similar to class F fly ash according to ASTM C593 (2006), is supplied by Nantong Power Plant, Jiangsu Province, China. River sand with fineness modulus of 2.6 and continuous grade crushed basalt stone with a maximum size of 20 mm are used as fine and coarse aggregates. A polycarboxylic-type superplasticizer with water reducing ratio of 25.8% is used, and the amount is adjusted to keep the slump of fresh concrete mixture in the range of 200–220 mm. The chemical composition and physical properties of raw materials are listed in Table 1.

2.2 Specimen preparation

A total of six batches are made in this study. The details of experimental program are given in Table 2. Batch “FA00I35” to batch “FA60I35” are used to compare the influence of fly ash content (0%, 20%,

Table 1 Chemical composition and physical properties of raw materials

Raw material	Chemical composition (%)								Specific surface area (m^2/kg)	Water demand ratio (%)
	SiO_2	Al_2O_3	Fe_2O_3	TiO_2	CaO	MgO	SO_3	Loss		
PC	21.47	5.80	4.04	–	59.64	3.24	2.08	2.44	310	–
FA	45.38	33.53	5.29	4.71	3.16	2.81	0.43	5.30	345	95

PC: Portland cement; FA: Grade I fly ash

Table 2 Experimental program

Batch	Binder (kg/m^3)	Fly ash		Water to binder ratio	Workability (mm)		Mechanical strength at 28 d (MPa)	
		Type	Content (%)		Slump	Flowability	Compressive	Flexural
FA00I35	458	I	0	0.35	205	550	77.0	9.85
FA20I35	458	I	20	0.35	205	530	72.2	5.44
FA40I35	458	I	40	0.35	210	580	65.5	4.98
FA60I35	458	I	60	0.35	220	585	55.1	4.39
FA40I30	458	I	40	0.30	205	530	64.9	5.73
FA40I40	458	I	40	0.40	210	590	61.6	4.72

FAxxIyy: FAxx represents the fly ash content (xx), I represents Grade I fly ash, and yy represents water to binder ratio

40%, and 60%). Batches “FA40I30”, “FA40I35”, and “FA40I40” are specifically designed to investigate the effect of water to binder ratio (W/B) (0.30, 0.35, and 0.40). The mass ratio of sand-to-(sand+stone) is maintained at 0.385 for all the batches.

2.3 Experimental program

According to Chinese standard test method JTJ270-98 (1998) and the mixture proportions in Table 2, fresh concrete mixtures are made in a compulsory planetary mixer. Then cubic concrete specimens with a size of 70 mm×70 mm×250 mm are cast, and then kept at room temperature for 24 h. Thereafter, the cubic specimens are demoulded and cured under the conditions of (20±3) °C and ≥95% relative humidity (RH) for 28 d.

2.4 Method

2.4.1 Chloride ion diffusion test under flexural stress

Concrete specimens are taken from the curing room at 28 d, then are oven-dried at 60 °C for 48 h, and coated with gas-tight epoxy resin on the specified faces according to the 1D or 2D chloride ion diffusion, which is subsequently described in detail. The flexural stress is applied to the above treated specimens. After that, the preloading concrete specimens are placed together with the loading frame into chloride solution (NaCl solution: 350 g/L) for 1, 3, 6, 9, and 12 months, respectively. In order to keep the constant Cl^- concentration, the NaCl solution is refreshed every week for the first 3 months, and then refreshed every 3 weeks in the later 9 months. The temperature was kept constant at 20 °C throughout the entire test period. At the specified immersion period, the specimen is taken out and dried for 2 d at (20±3) °C and (50±5)% RH. The preloading frame is removed. Subsequently the powder samples at successive layers from different depths (0–5, 5–10, 10–15, and 15–20 mm, respectively, from the external surface), are obtained by drilling the specimen along 1D and 2D diffusion directions. The coarse particles are removed through a 0.63 mm sieve. The fine powders are used to determine the free and total Cl^- concentrations of the concrete specimen by employing the chemical titration methods in compliance with Chinese standard test method JTJ270-98 (1998). The keys in this study are the external stress application and 2D Cl^- diffusion.

1. Preloading frame and flexural stress application

In this study, a spring type of preloading frame is specially designed to accurately apply external flexural stress to concrete specimens, as shown in Fig. 1. The frame is made of stainless steel, and the load which is applied comes from elastic forces of spring compression (Zhang *et al.*, 2007). Before applying flexural stress, the beam concrete specimens are firstly placed in the preloading frame (the support span is 210 mm on the bottom, 70 mm on the top, respectively) according to Fig. 1, then applying flexural stress by using MTS810 materials testing machine (MTS Systems Corporation, USA) at a rate of 0.01 mm/s. When the specified stress ratio, i.e., the ratios of externally applied flexural load to the ultimate flexural load capacity, is reached, the MTS810 machine is immediately stopped and the screw caps are tightly screwed.

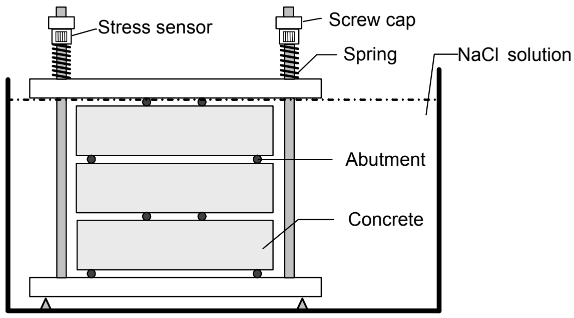

Fig. 1 Sketch of the preloading concrete subjected to 1D and 2D chloride ion attacks

The flexural stress is monitored in real time by the stress sensors connected with computer. Once the stress loss exceeds 3%, it will be restored to the original one through screwing the caps. In this study, five flexural stress ratios (0.20, 0.35, 0.50, 0.65, and 0.80) are applied to batch FA40I40 (28 d), while only the stress ratio of 0.35 is applied to the other batches.

2. 1D and 2D stress-diffusion test

(1) 1D stress-diffusion

Concrete specimens are coated with epoxy on five faces (two end faces, the forming face, one bottom face, and one side face), leaving free one side face to be exposed to the combination actions of NaCl solution and flexural stress. When the chloride ion immersion test reaches the specified exposure periods, chloride sampling was undertaken by drilling the specimen on the free face at the middle region, as shown in Fig. 2a. The powder samples are collected from the surface to the inner region of the specimens at 5-mm intervals using a diamond aiguille. At least 5 g of fine powders are required to measure the free and total Cl^- contents of each layer concrete.

The chloride analysis was undertaken according to JTJ270-98 (1998), similar to ASTM C1152 (2004) and ASTM C1218 (2008) for free and total chloride concentrations, using the Volhard titration method (NT Build 208, 1996). The chloride content is always expressed as percent Cl^- by mass of concrete. The chloride content was plotted against the distance from the concrete surface, presenting the chloride penetration profile in concrete.

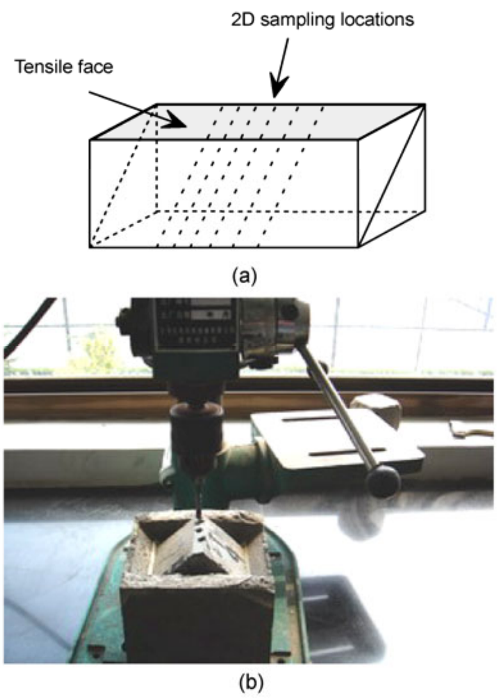

Fig. 2 2D sampling location (a) and 2D sampling (b)

(2) 2D stress-diffusion

2D accelerated Cl^- diffusion test is similar to the 1D diffusion. The differences between 1D and 2D are as follows: for 2D stress-diffusion test, the concrete specimen is coated with epoxy on four faces (two end faces, the forming face, and one side face), leaving free two vertical side faces to be exposed to NaCl solution and flexural stress action. One free side face is used to bear tensile stress. The preloaded specimens are immersed in NaCl solution. At specified exposure periods, the specimens are taken out, and the preloading frames are removed. Subsequently the specimens are placed into a specially machining fixture to ensure that the powder samples are always drilled along the diagonal face (<45°) of the specimen, i.e., 2D direction, as shown in Fig. 2b. The free and total chloride contents are obtained by titrating the collected fine powder samples in compliance with Chinese standard test method JTJ270-98 (1998).

2.4.2 In-situ observation of microcracks prorogation under stress

In order to investigate the mechanism of chloride ion accelerating effect caused by the external flexural stress, a small-sized loading frame with a length of 50 mm, width of 20 mm, and height of 50 mm is also manufactured for in-situ observation of the whole process of the initiation, prorogation, and distribution of microcracks in the flexural zone of specimen under different stress ratios (Zhang *et al.*, 2007), as shown in Fig. 3. The frame is so small that it can be placed in the sample chamber of the scanning electron microscope (SEM). The specimen of 10 mm×10 mm×40 mm is made with the mortar taken from batch "FA40I35" excluding the coarse aggregates. In order to easily find the same locations at different observations, the grid of 1 mm×1 mm is drawn on the tensile faces of the mortar specimen with black ink pen (Fig. 4). When performing the SEM observation, the microcracks distribution is firstly observed on the surface of the specimen without stress. Then, the specimen is taken from the chamber of SEM and placed in the small-sized frame. The flexural stress with the stress ratio of 0.2 is applied by screwing the bolt with one slot on the top surface. The stress ratio is controlled by the compression length. The preloaded specimen is

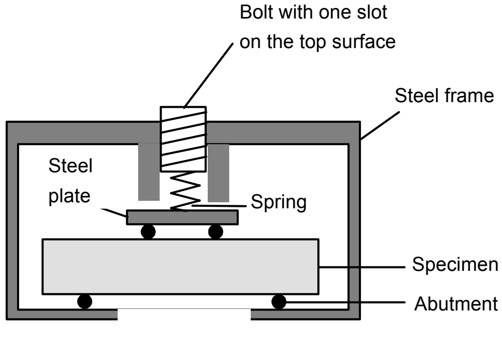

Fig. 3 Sketch of the small-sized preloading setup

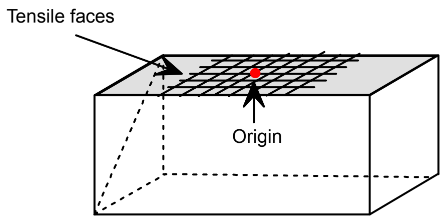

Fig. 4 Microcracks observation locations on the tensile faces of specimen under flexural stress

taken back the SEM chamber and the microcracks are observed at the same locations. Then the flexural stress with the ratio of 0.35 is applied by further screwing the bolt, and then SEM observation is conducted. In an orderly way the flexural stress ratio of 0.80 is reached. The typical image, size and distribution of microcracks are compared on the tensile faces of specimen at the same locations with different stress ratios.

3 Results and discussion

1D and 2D chloride ion diffusion behaviors of the fly ash concretes under flexural stress are systematically investigated at different NaCl immersion ages of 1, 3, 6, 9, and 12 months, respectively.

3.1 Effect of fly ash content

Fly ash content plays an important role in stress-diffusion of fly ash concrete. The effects of fly ash contents on 1D and 2D stress-diffusion with the stress ratio of 0.35 are illustrated in Figs. 5a and 5b, respectively.

It can be seen from Fig. 5 that both 1D and 2D Cl^- diffusion under stress exhibit a rapidly decreasing trend with an increase in the distance from the surface for various fly ash concretes. Compared to the concrete without fly ash, the free chloride ion concentration in fly ash concrete is clearly reduced. When fly ash content is less than 40%, fly ash addition clearly reduces the chloride ion diffusion, resulting in low free chloride ion concentration in various distances excluding the first layer of fly ash concrete compared with the concrete without fly ash, as shown in Fig. 5. The free chloride ion content in the first layer (0–5 mm) is easily misjudged due to carbonation of the surface layer concrete. Thus, when analyzing chloride ion diffusion behavior, the data in the surface layer is often discarded. When too much fly ash (60%) is incorporated, the compressive strength is greatly reduced. About 28% strength loss can be observed, as shown in Table 2. The porosity is also considerably increased (Fig. 6). As a result, the chloride ion diffusion coefficients show an incremental trend (Table 3). The chloride ion easily transports into the concrete with high volume fly ash.

3.2 Effect of water to binder ratio

W/B also exhibits a great impact on stress-diffusion of fly ash concrete. The effects of W/B on 1D and 2D stress-diffusion are illustrated in Figs. 7a and 7b in the stress ration of 0.35, respectively.

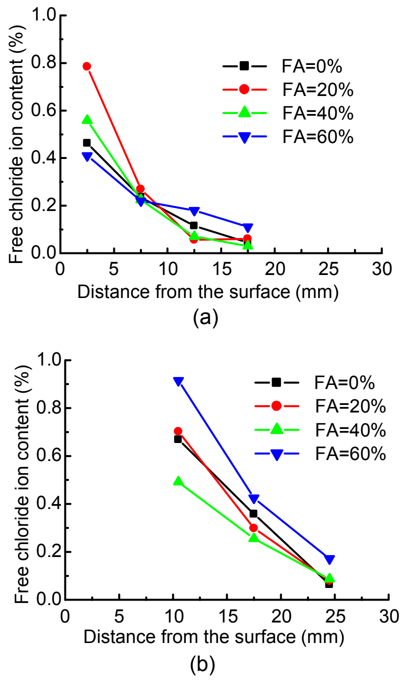

Fig. 5 Effect of fly ash content (FA) on 1D (a) and 2D (b) chloride ion diffusion of concrete under flexural stress with the stress ratio of 0.35

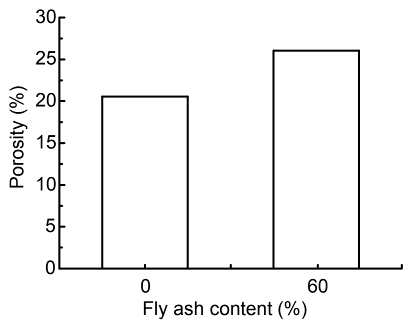

Fig. 6 Effect of fly ash content on porosities of concrete

It can be seen from Fig. 7 that when fly ash content is kept constant (40%), Cl^- diffusion concentration despite 1D and 2D clearly increases with an increase in W/B. It is especially true for W/B ranging from 0.30 to 0.35. When W/B varies from 0.35 to 0.40, an increase in W/B will have comparatively little influence on the Cl^- diffusion. Cl^- diffusion coefficients of fly ash concrete with different W/B also exhibit a similar trend. This may be attributed to an increase in porosity caused by the high W/B (Fig. 8), resulting in a rapid Cl^- diffusion.

Table 3 Chloride ion diffusion coefficients of various fly ash concrete in the flexural stress with the ratio of 0.35 and six month immersion

Batch	Effective chloride ion diffusion coefficient ($\times10^{-8}$ cm^2/s)	
	1D	2D
FA00I35	7.1	13.9
FA20I35	3.0	12.3
FA40I35	3.9	7.5
FA60I35	12.0	23.5
FA40I30	3.4	6.8
FA40I40	4.7	9.2

FAxxIyy: FAxx represents the fly ash content (xx), I represents Grade I fly ash, and yy represents water to binder ratio

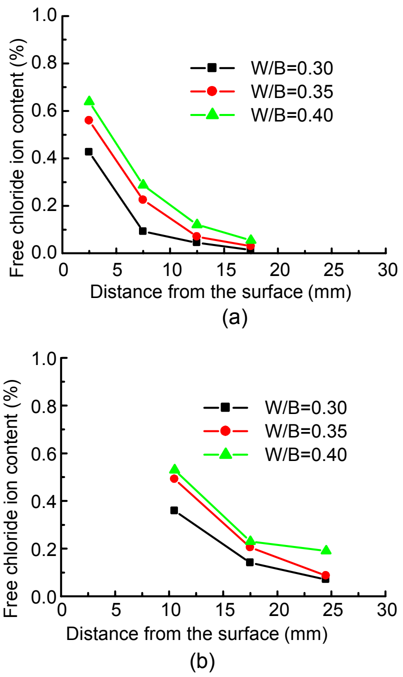

Fig. 7 Effect of water to binder ratio on 1D (a) and 2D (b) chloride ion diffusion of concrete under flexural stress with the stress ratio of 0.35

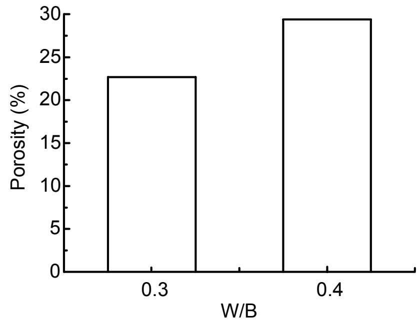

Fig. 8 Effect of W/B on porosities of concrete

3.3 Effect of dimensions on stress-diffusion

The effect of dimensions on stress-diffusion of fly ash concrete is shown in Fig. 9. Theoretically, if there is no diffusion interaction effect, 2D Cl^- concentration of the edge concrete at the same distance should be $\sqrt{2}$ times larger than 1D Cl^- concentration. However, the experimental results show that 2D Cl^- concentration is much larger than the theoretical one, as shown in Fig. 9. In addition, 2D chloride ion diffusion profile does not exhibit an orthogonal angle outline, but a round one, as shown in Fig. 10. All these indicate the existence of an obvious dimensional interaction effect, resulting in rapid chloride ion transportation in 2D diffusion zone. Thus, more attention should be paid to the 2D stress- diffusion of the edge locations of concrete structures, especially for long-span beams in flexural or tensile stress state. The chloride ion diffusion rate and depth of these locations are much larger than 1D diffusion of the other locations. The steel bars embedded in these locations subjected to combined actions of 2D chloride ion flow and flexural stress firstly suffer from corrosion, which will become an important deterioration resource.

3.4 Effect of stress ratios

Flexural stress ratios show important influence on the chloride ion diffusion of fly ash concrete. Fig. 11 shows the 1D and 2D chloride ion diffusion behaviors of fly ash concrete made with 40% fly ash (FA40I35) subjected to different flexural stress ratios of 0, 0.20, 0.35, 0.50, 0.65, and 0.80, respectively.

It can be seen through a comparison of 1D and 2D chloride ion diffusion of fly ash concrete between those in loading state and non-loading state that stress-diffusion is considerably larger than non-stress

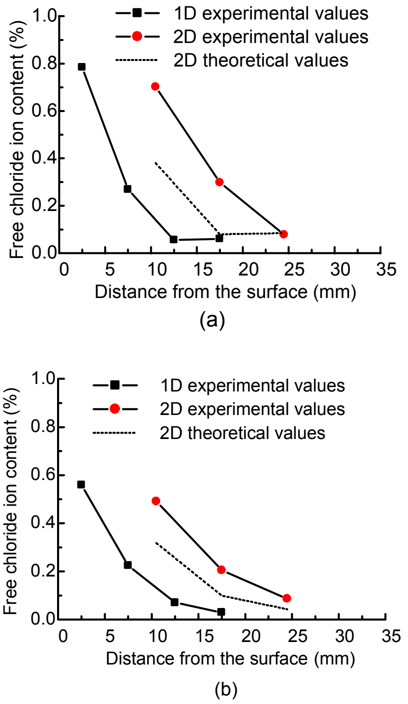

Fig. 9 Effect of dimensions on chloride ion diffusion of fly ash concrete under flexural stress
(a) FA20I35 (b) FA40I35

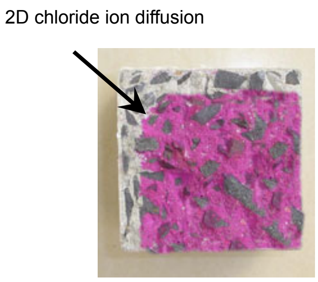

Fig. 10 2D chloride ion diffusion profile

diffusion, i.e., flexural stress accelerates the chloride ion diffusion. The accelerating effect is more obvious with the development of immersion ages. In addition, higher stress ratios show faster chloride ion diffusion. However, cracks are not seen on the tensile faces of the specimen in the stress range employed in this study. To know the possible reason that leads to the rapid chloride ion diffusion of fly ash concrete in the stress state, the microstructure of the tensile faces is observed and compared on the specimen at the same locations with different stress ratios (Fig. 12).

It can be clearly seen that the microstructure becomes relatively loose for the specimen in the stress state. Some microcracks are initiated, as shown in the rectangular section of Fig. 12. The size of microcracks also gradually increases with an increase in the stress (Table 4). This indicates that some defects existed in the concrete matrix, such as pore, air bubble, and microcracks, which will further increase and develop in the stress state and become accessible pathways of aggressive medium. Hence, the reason for stress accelerating diffusion is mainly that the external flexural loading accelerates the initiation and propagation of microcracks, and increases the amount and size of microcracks in tensile zone, resulting in chloride ion rapidly penetrating into the concrete. Since it is quite difficult to characterize

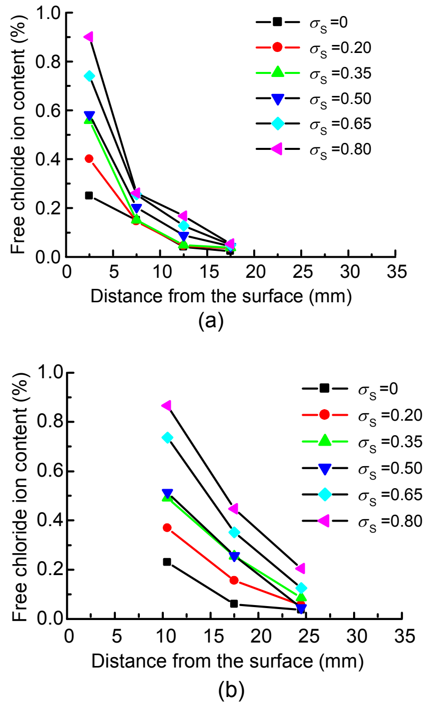

Fig. 11 Effect of stress ratios (σ_S) on 1D (a) and 2D (b) chloride ion diffusion of concrete

Table 4 Microcrack size development on the tensile faces of specimen under different stress ratios

Stress ratio	Length (μm)	Width (μm)
0.2	31	16
0.35	32	19
0.5	34	21
0.6	37	21
0.8	42	27

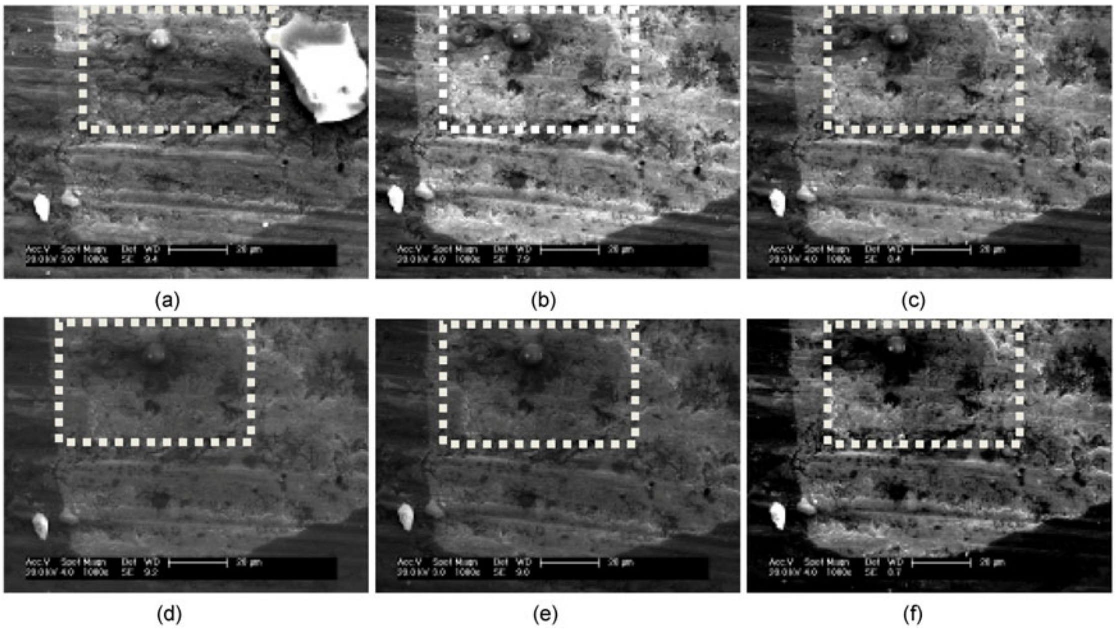

Fig. 12 In-situ SEM observations of the microcrack prorogation on the tensile faces of specimen under different stress ratios: 0 (a), 0.2 (b), 0.35 (c), 0.50 (d), 0.65 (e), and 0.80 (f)

the microcracks network in tensile zone, the externally applied flexural stress ratio σ_S is chosen as the main parameter reflecting the microcracks network in a loading state. Moreover, σ_S can be a durability criterion as a threshold microscopic for damage of the concrete.

In order to quantify the chloride ion diffusion accelerating effect caused by the external flexural stress, a stress accelerating factor is proposed and defined as follows:

$$K_{\sigma_S} = \frac{D_{\sigma_S}}{D_0}, \tag{1}$$

where D_{σ_S} is the chloride ion diffusion coefficient of concrete in loading state with flexural stress ratio of σ_S, and D_0 is the chloride ion diffusion coefficient of concrete in non- loading state.

Fig. 13 illustrates the relationship between the stress accelerating factor (K_{σ_S}) and the flexural stress ratios (σ_S). It can be observed that K_{σ_S} is a function of σ_S. At low stress ratios, K_{σ_S} exhibits a comparatively small increase with an increase in σ_S. At higher stress ratios, K_{σ_S} shows a rapid increase with an increase in σ_S. An exponential relationship $K_{\sigma_S} = 1 + 0.51\sigma_S^{0.6}$ can be found through regression of experimental results, as shown in Fig. 13.

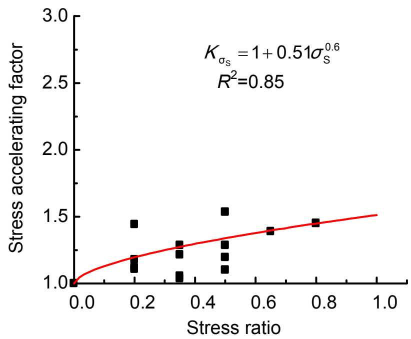

Fig. 13 Relationship between the stress accelerating factor and the flexural stress ratios

4 Conclusions

1. Compared to 1D nonstress-diffusion, 2D chloride ion diffusion of fly ash concrete in flexural loading state exhibits a much larger diffusion rate. This will lead to more serious stress-corrosion in the edge locations of long-span beams in fly ash concrete structures exposed to chloride ion environment. Thus,

the steel bars embedded in these locations will be prone to suffer from chloride ion attack and begin to initiate corrosion.

2. Fly ash content and W/B have great impact on 1D and 2D chloride ion diffusion of fly ash concrete in loading state. Stress-diffusion will increase with an increase in fly ash content. A reduction in W/B is helpful for enhancing the resistance to stress-diffusion attack.

3. Flexural stress accelerates 1D and 2D chloride ion diffusion of fly ash concrete. The stress accelerating factor K_{σ_S} increases with an increase in stress ratio σ_S. An exponential relationship $K_{\sigma_S}=1+0.51\sigma_S^{0.6}$ between K_{σ_S} and σ_S can be found through regression of experimental results.

References

ASTM C1152, 2004. Standard Test Method for Acid-Soluble Chloride in Mortar and Concrete. ASTM International, West Conshohocken, PA, USA.

ASTM C1218, 2008. Standard Test Method for Water-Soluble Chloride in Mortar and Concrete. ASTM International, West Conshohocken, PA, USA.

ASTM C150, 2005. Standard Specification for Portland Cement. ASTM International, West Conshohocken, PA, USA.

ASTM C593, 2006. Standard Specification for Fly Ash and Other Pozzolans for Use with Lime for Soil Stabilization. ASTM International, West Conshohocken, PA, USA.

Chalee, W., Teekavanit, M., Kiattikomol, K., Siripanichgorn, A., Jaturapitakkul, C., 2007. Effect of W/C ratio on covering depth of fly ash concrete in marine environment. *Construction and Building Materials*, **21**(5):965-971. [doi:10.1016/j.conbuildmat.2006.03.002]

Chindaprasirt, P., Chotithanorm, C., Cao, H.T., Sirivivatn, V., 2007. Influence of fly ash fineness on the chloride penetration of concrete. *Construction and Building Materials*, **21**(2):356-361. [doi:10.1016/j.conbuildmat.2005.08.010]

Choi, Y.S., Kim, J.G., Lee, K.M., 2006. Corrosion behavior of steel bar embedded in fly ash concrete. *Corrosion Science*, **48**(7):1733-1745. [doi:10.1016/j.corsci.2005.05.019]

Darmawan, M.S., 2010. Pitting corrosion model for reinforced concrete structures in a chloride environment. *Magazine of Concrete Research*, **62**(2):91-101. [doi:10.1680/macr.2008.62.2.91]

Dhir, R.K., Jones, M.R., 1999. Development of chloride-resisting concrete using fly ash. *Fuel*, **78**(2):137-142. [doi:10.1016/S0016-2361(98)00149-5]

Friedmann, H., Amiri, O., Ait-Mokhtar, A., Dumargue, P., 2004. A direct method for determining chloride diffusion coefficient by using migration test. *Cement and Concrete Research*, **34**(11):1967-1973. [doi:10.1016/j.cemconres.2004.01.009]

Friedmann, H., Amiri, O., Ait-Mokhtar, A., 2008. Physical modeling of the electrical double layer effects on multispecies ions transport in cement-based materials. *Cement and Concrete Research*, **38**(12):1394-1400. [doi:10.1016/j.cemconres.2008.06.003]

GB175, 2007. Common Portland Cement. State General Administration of the People's Republic of China for Quality Supervision and Inspection and Quarantine, Beijing, China (in Chinese).

GB/T1596, 2005. Fly Ash Used for Cement and Concrete. State General Administration of the People's Republic of China for Quality Supervision and Inspection and Quarantine, Beijing, China (in Chinese).

JTJ270-98, 1998. Testing Code of Concrete for Port and Waterwog Engineering. Ministry of Communications of China, Beijing, China (in Chinese).

Khatri, R.P., Sirivivatnanon, V., 2004. Characteristic service life for concrete exposed to marine environments. *Cement and Concrete Research*, **34**(5):745-752. [doi:10.1016/S0008-8846(03)00086-3]

Liang, M.T., Wang, K.L., Liang, C.H., 1999. Service life prediction of reinforced concrete structures. *Cement and Concrete Research*, **29**(9):1411-1418. [doi:10.1016/S0008-8846(99)00109-X]

Liang, M.T., Huang, R., Feng, S.A., 2009. Service life prediction of pier for the existing reinforced concete bridges in chloride-laden environment. *Journal of Marine Science and Technology-TAIWAN*, **17**(4):312-319.

Maage, M., Helland, S., Poulsen, E., 1996. Service life prediction of existing concrete structures exposed to marine environment. *ACI Materials Journal*, **93**(6):602-608.

Mehta, P.K., 1997. Durability—critical issues for the future. *Concrete International*, **19**(7):27-33.

Mien, T.V., Stitmannaithum, B., Nawa, T., 2009. Simulation of chloride penetration into concrete structures subjected to both cyclic flexural loads and tidal effects. *Computers and Concrete*, **6**(5):421-435.

Montemor, M.F., Cunha, M.P., Ferreira, M.G., Simões, A.M., 2002. Corrosion behavior of rebars in fly ash mortar exposed to carbon dioxide and chlorides. *Cement and Concrete Composites*, **24**(1):45-53. [doi:10.1016/S0958-9465(01)00025-7]

NT Build 208, 1996. Concrete, Hardened: Chloride Content by Volhard Titration. Nordtest, Tekniikantie, Espoo, Finland.

Rukzon, S., Chindaprasirt, P., 2008. Mathematical model of strength and porosity of ternary blend Portland rice husk ash and fly ash cement mortar. *Computers and Concrete*, **5**(1):75-88.

Rukzon, S., Chindaprasirt, P., 2009. Strength and chloride penetration of Portland cement mortar containing palm oil fuel ash and ground river sand. *Computers and Concrete*, **6**(5):391-401.

Suwito, C., Xi, Y., 2008. The effect of chloride-induced steel corrosion on service life of reinforced concrete structures.

Structure and Infrastructure Engineering, **4**(3):177-192. [doi:10.1080/15732470600688699]

Tang, L.P., Nilsson, L.O., 1993. Rapid determination of the chloride diffusivity in concrete by applying an electrical field. *ACI Materials Journal*, **89**(1):49-53.

Thomas, M.D.A., Bamforth, P.B., 1999. Modelling chloride diffusion in concrete effect of fly ash and slag. *Cement and Concrete Research*, **29**(4):487-495. [doi:10.1016/S0008-8846(98)00192-6]

Weyers, R.E., 1998. Service life model for concrete structures in chloride laden environments. *ACI Materials Journal*, **95**(4):445-453.

Zhang, Y.S., Sun, W., Chen, S.D., Guo, F., Zhao, Q.X., 2007. 1D and 2D carbonation of fly ash concrete under flexural stress. *Journal of Southeast University (Natural Science Edition)*, **37**(1):118-122 (in Chinese).

Zhang, Y.S., Sun, W., Chen, S.D., Li, Z.J., 2011. Two and three dimensional chloride ingress into fly ash concrete. *Journal of Wuhan University of Technology-Materials Science Edition*, in Press.